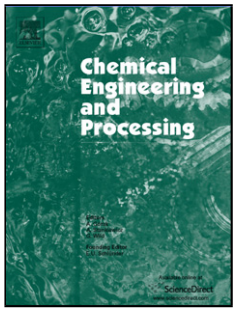

Title: Quantitative Analysis of Hydrodynamic Effect on Transesterification Process in T-junction Microchannel Reactor System

Authors: Afiq Mohd Laziz, Ku Zilati Ku Shaari, Jitkai Chin, Jens Denecke

PII: S0255-2701(18)31131-0
DOI: https://doi.org/10.1016/j.cep.2019.04.019
Reference: CEP 7519

To appear in: *Chemical Engineering and Processing*

Received date: 20 September 2018
Revised date: 22 April 2019
Accepted date: 29 April 2019

Please cite this article as: Mohd Laziz A, Ku Shaari KZ, Chin J, Denecke J, Quantitative Analysis of Hydrodynamic Effect on Transesterification Process in T-junction Microchannel Reactor System, *Chemical Engineering and Processing - Process Intensification* (2019), https://doi.org/10.1016/j.cep.2019.04.019

Quantitative Analysis of Hydrodynamic Effect on Transesterification Process in T-junction Microchannel Reactor System

Afiq Mohd Laziz[a], Ku Zilati Ku Shaari[a,*], Jitkai Chin[b], Jens Denecke[c]

[a] Chemical Engineering Department, Universiti Teknologi PETRONAS, 32610 Bandar Seri Iskandar, Perak, Malaysia.

[b] School of Applied Sciences, University of Huddersfield, Queensgate, HD3 3JL, Huddersfield, United Kingdom.

[c] Institute of Refrigeration, Air-Conditioning, and Environmental Engineering, Karlsruhe University of Applied Sciences, 76133 Karlsruhe, Germany.

*Corresponding author. Email address: kuzilati_kushaari@utp.edu.my

Graphical abstract

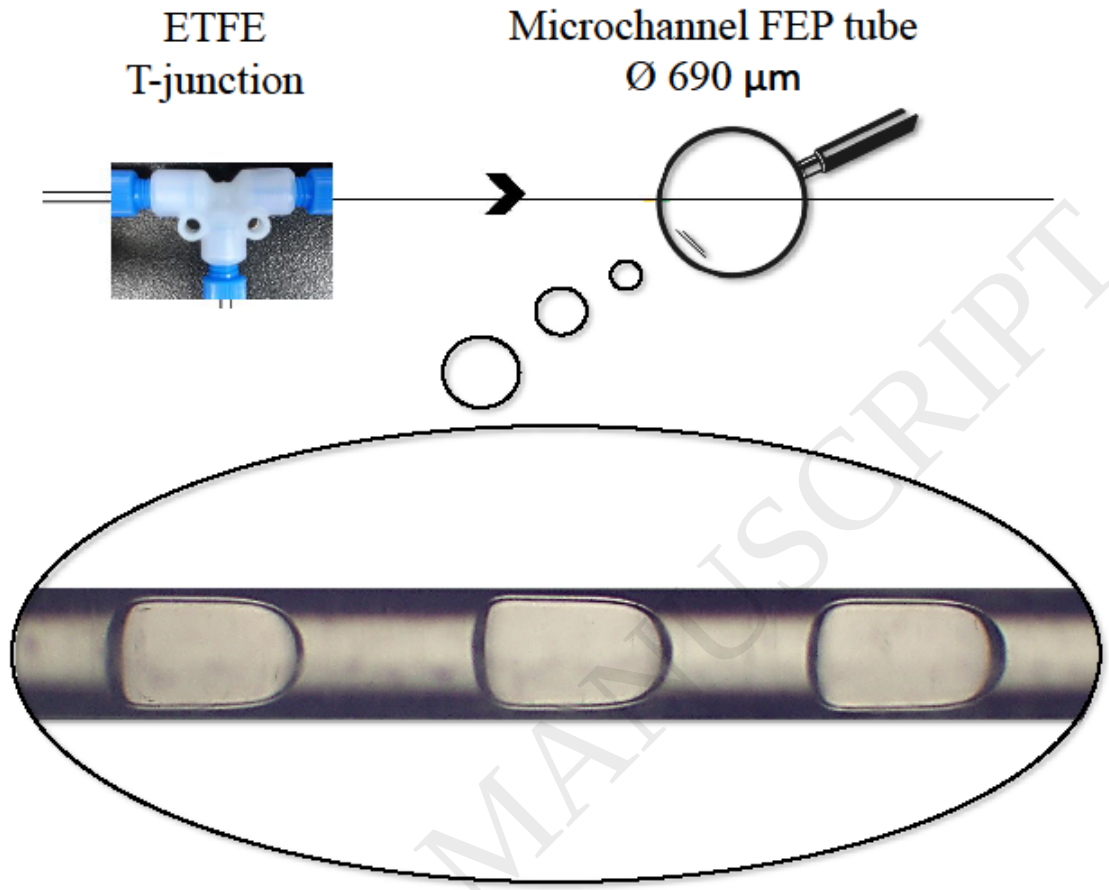

Highlights

- Effect of CH_3OH slugs size & methanol/oil ratio is studied on oil conversion.
- Biodiesel oil and methanol are separated inline by using a membrane separator.
- 98% oil conversion is achieved at room temperature in 80 seconds.
- Additional factor of number of slugs enhances the oil conversion.
- Recirculation pattern is observed in slug by experiment and CFD method.

Abstract

Microfluidic technology offers high interfacial area particularly in the multiphase reaction such as transesterification process to produce biodiesel. Methanol-to-oil molar ratio is one of the important parameters to enhance the biodiesel production. However, very few in literature are focusing on the hydrodynamic effect that is caused by the molar ratio accurately. In this study, stable and highly consistent droplet-slug flow inside a microchannel was generated using a T-junction to investigate the impact of hydrodynamic factor on the reaction. High molar ratio creates high interfacial area and number of droplets, hence resulting in the highest conversion of oil. This finding has revealed that it is possible to obtain 98% oil conversion at room temperature and relatively short reaction time of 80 s. It demonstrates that microchannel reactor has high potential for intensified process in the production of biodiesel.

Keyword: *Biofuel, microfluidic, passive mixing, CFD, multiphase.*

1. Introduction

Renewable source of energy such as biodiesel has received a good acceptance worldwide to reduce the dependence on fossil fuels and protect the environment. The common process to produce biodiesel involves the use of triglyceride (TG) either from vegetable or animal oil with alcohol and the basic catalyst (i.e. potassium hydroxide, KOH) to produce fatty acid methyl ester (FAME) and glycerol (a byproduct); also known as transesterification process. As the reaction concludes, two distinct phases are formed; the oil phase and the aqueous phase. The oil phase consists of the biodiesel and the unreacted triglycerides while the aqueous phase consists of glycerol and unreacted alcohol. Process intensification can be defined as any chemical engineering development that leads to substantially smaller, cleaner, safer, and more energy efficient

technology (Stankiewicz and Moulijn, 2000). Although transesterification has been widely studied, process intensification in biodiesel production is the new trend that run the process continuously, reduce the reaction time and use a lower amount of catalyst (Tiwari et al., 2018). A simple modular design or 'plug & play' microreactor is possible by using a common transparent capillary tube for microchannel, with manifold junctions as the droplet generators. This method is not only fast and easy to assemble, but it also has significant flexibility to change the microchannel design in terms of total length, internal diameter, channel configuration, and number of junction manifolds. This concept has a bright future for the upscaling of microreactor and intensification of biodiesel production (Billo et al., 2015).

Many studies have been carried out to investigate the transesterification process using microreactors (Guan et al., 2009; Jamil et al., 2016; Rahimi et al., 2014; Wen et al., 2009). According to the optimization study by Rahimi *et* al., the most important parameter to improve biodiesel production is the methanol-to-oil molar ratio. This parameter is mostly related to the mass transfer of reactants and the probability of the reactants to have contact and undergo a chemical reaction. Transesterification process is a multiphase reaction because both reactants are immiscible to each other and the reaction rate can be limited by mass transfer across the interface of both phases. Since KOH is insoluble in the oil phase, the reaction occurs only inside the methanol phase (Csernica and Hsu, 2012), which is the focus in this study to investigate the hydrodynamic characteristics of the methanol phase. Depending on the flow conditions, flow regimes such as slug and droplet flow can be formed in a multiphase flow (Xu et al., 2008). Although the effect of methanol-to-oil molar ratio on the conversion of oil were reported, there is no concrete explanation on the reason behind the results obtained. Rashid *et* al. found that the biodiesel yield increases as the methanol-to-oil molar ratio increases up to 23 (Rashid et al., 2014).

Other researchers found a molar ratio of 9 as an optimum value for the best reaction performance (Aghel et al., 2014; Santana et al., 2017, 2016; Tanawannapong et al., 2013). Despite the differences in their results, only few researchers have reported the hydrodynamics observation for their multiphase flow regime. One noticeable problem in the flow of a transesterification reaction is the inconsistent flow regime that is probably due to the existence of quasi-homogeneous phase and the effect of agglomeration inside the microchannel (Guan et al., 2009). To the contrary, in their observation, when the flow was under room temperature, the flow regime became interestingly more stable. Having a process at room temperature is a great advantage in the industry because it will not only make the process safer and economical but also reduce the complexity of the entire design.

Computational fluid dynamics (CFD) is a branch of fluid mechanics to investigate the physical phenomena governing fluid flow using numerical analysis and data structures. It can help in solving the complex flow problems especially when it is hard to see with naked eyes what's going on in the process reactor (Mohd Tamid et al., 2011). Santana et al. applied the CFD analysis in their design optimization of microchannel for biodiesel synthesis (Santana et al., 2019a). The introduction of obstruction with different types of geometry such as triangular baffle (Santana et al., 2019b) or circular obstruction (Santana et al., 2018) further enhance the mixing of oil and alcohol in the microchannel reactor with the help of a CFD tool (Elsholkami et al., 2016). Some other numerical studies that include the mass transfer mechanism for transesterification process are also reported (Noriega et al., 2017; Pontes et al., 2016). However, most of the CFD analyses in the microchannels resulted in a stratified flow regime. Jamil et al. observed that the slug/droplet flow results in the higher FAME yield as compared to stratified/parallel flow in the microchannel (Jamil et al., 2016). To the best of authors' knowledge, no CFD modelling of the slug/droplet flow

in microchannel for transesterification process is reported in the literature. Therefore, the simulation of the slug flow will be explored and investigated in this study.

In this paper, the study focuses on the effect of hydrodynamic parameters such as the interfacial area and the number of droplets on the production of biodiesel in a T-junction microchannel reactor. The effect of methanol-to-oil molar ratio on the multiphase flow regime, such as the droplet length, diameter, and distance are experimentally investigated by the characterization under the microscope. While the reaction conditions such as the temperature, residence time, and the total volumetric flow rate were kept constant, different oil conversions were achieved at different methanol-to-oil ratios. The results were supported by the CFD simulation for the description of the hydrodynamic characteristics inside the slug, specifically on the internal recirculation zones, velocity and concentration contours. To further enhance the continuous process, a membrane separation technique was used to instantly separate the biodiesel product from the glycerol by-product. The study also demonstrates the importance of hydrodynamic effect of the reaction and its feasibility to synthesize biodiesel using a modular 'plug & play' microreactor at room temperature, which can inspire future development of large-scale continuous process biodiesel production.

2. Materials and Methods

2.1 Materials and Chemicals

The oil phase was a refined, food-grade cooking palm oil from Buruh® manufactured by Lam Soon Sdn. Bhd. (Selangor, Malaysia). The physical properties of the oil at room temperature (25°C) are as follows: a density of 909.15 $kg.m^{-3}$, a viscosity of 0.0691 Pa.s, and an interfacial tension with methanol of 3.27 $mN.m^{-1}$. Methanol was purchased from QReC® (Selangor, Malaysia) with analysis reagent standard. Potassium hydroxide (KOH) pellets, 2-propanol, methyl

oleate, and n-hexane were purchased from Merck® (Darmstadt, Germany). Transparent fluorinated ethylene propylene (FEP) capillary tube with an inner diameter of 690 µm was used as a microchannel reactor for transesterification reaction and observation of the droplet characteristics. Transparent polytetrafluoroethylene (PTFE) Teflon tube with inner diameter of 800 µm was used as a fluid carrier from the reservoir container to the T-junction. Ethylene tetrafluoroethylene (ETFE) Luer Lock T-junction was used as a droplet generator that merges two phases into the microchannel reactor. Aeos® ePTFE was used for the membrane separator supplied by Zeus® (Letterkenny, Ireland).

2.2 Experimental Setup for Transesterification Reaction

A schematic diagram of the experimental set-up for slug characteristics and transesterification reaction is depicted in Fig.1.

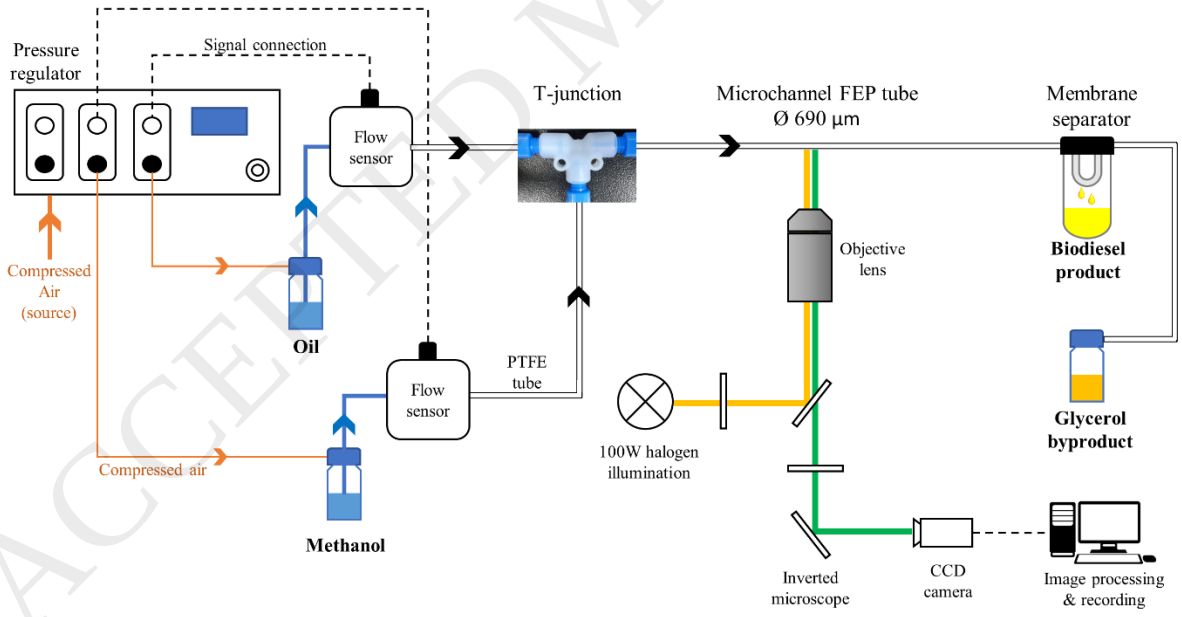

Fig. 1. Schematic diagram of the complete experimental setup.

A high precision pressure pump system from Elveflow® (Paris, France) was used to individually control the flow rates of the palm oil and methanol, driven by compressed air. PTFE tubes were used to navigate the flow of methanol and oil to the T-junction. A transparent FEP capillary tube, the 'microchannel reactor', is attached directly downstream of the ETFE T-junction. The microchannel has a total length of 1-meter, and the slug size was measured at every 20 cm from the T-junction and different time to assure slug reproducibility. The transesterification reaction takes place immediately after the junction where the two reactants meet. To study the effect of methanol-to-oil molar ratio on the transesterification reaction, the individual volumetric flow rates of methanol and oil were controlled as described in Table 1.

Table 1
Conversion of molar to volumetric flow rate ratio and corresponding individual inlet flow rate.

Molar ratio of methanol to oil	Volumetric ratio of methanol to oil	Oil flow rate, Q_{Oil} [$\mu L.min^{-1}$]	Methanol flow rate, Q_{MeOH} [$\mu L.min^{-1}$]
3.3	0.14	87.50	12.50
4.6	0.20	83.33	16.67
7.6	0.33	75.00	25.00
10.0	0.45	69.13	30.87
15.0	0.67	59.89	40.11
20.0	0.89	52.83	47.17
22.9	1.02	49.44	50.56

All the reaction parameters such as temperature (25°C), total volumetric flow rate (100 $\mu L.min^{-1}$), catalyst concentration (5 wt% KOH), and residence time (80 seconds) were kept constant for all

the cases. The total volumetric flow rate was calculated based on the sum of both individual methanol and oil flow rate, and the flow rates were kept constant to maintain identical residence time (80 seconds) for the reaction. The flow regimes and slug characteristics inside the microchannel were observed using Olympus inverted microscope IX53 equipped with a DP22 microscope CCD camera. The slug size was then measured from the captured image using cellSens Dimension software.

A membrane separation technique was used in this study to separate the biodiesel product and other components. The separation takes place due to the superior wettability of oil phase with the PTFE based membrane, the biodiesel separated easily from the aqueous phase that flows downstream of the channel. To enhance the separation performance, a stainless-steel tubing was inserted at the membrane outlet to promote the flow of the methanol phase because it has superior wettability with stainless-steel as compared to the oil phase. The oil phase collected in the product container was then analyzed for its biodiesel content. This physical separation method is beneficial as part of process intensification because the membrane can be replaced easily, energy neutral and zero waste production.

2.3 Biodiesel Content Analysis

After the collection of biodiesel product from the membrane separator, the samples were analyzed to check the biodiesel content according to the method suggested elsewhere (Nguyen et al., 2016). 50 μL of the sample was taken into a vial and diluted with 3 mL of the mobile phase that contains a mixture of n-hexane and iso-propanol of 97/3 volume ratio (*v/v*). The mixture was then mixed adequately by a vortex mixer. Subsequently, the oil concentration in the samples was analyzed by high-performance liquid chromatography equipped with a refractive index detector (HPLC-RID), from Shimadzu RID-10A (Japan). The same mobile phase during sample

preparation was used in the HPLC analysis. The separation column was a Shim Pack CLC-SIL (M) – (150 x 4.6 mm, 5 µm) and its temperature was maintained at 40°C. Methyl oleate was used as an internal standard for the calibration of biodiesel content. The oil conversion was defined as

$$Oil\ conversion\ (\%) = \frac{TG_{Initial}\ (mg) - TG_{Final}\ (mg)}{TG_{Initial}\ (mg)} \times 100 \quad (1)$$

2.4 Calculation of Interfacial Area

The calculation of surface area-to-volume (*S/V*) ratio was calculated based on the total interfacial area from the generated slugs over the volume of the entire microchannel. The constant volume of the microchannel was calculated for a total length of 1 m and an internal diameter of 690 µm using the simple formula for a cylindrical shape ($\pi D^2 L/4$). Three parameters were measured for the calculation of *S/V* ratio that includes the slug length, *L*, diameter, *D*, and distance, *d*, as illustrated in Fig. 2. The volume domain, *V*, can be described as the volume occupied by a single slug.

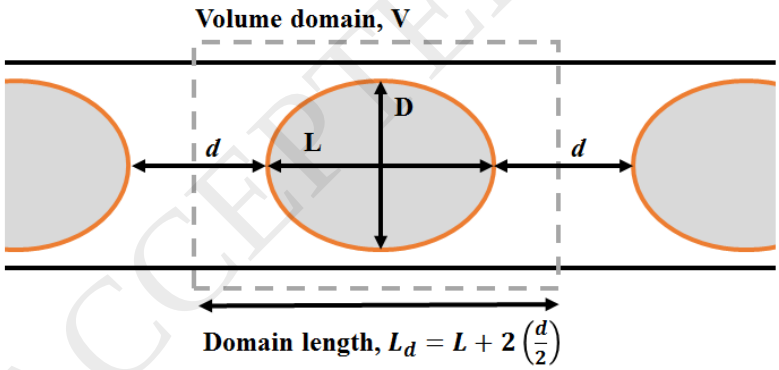

Fig. 2. Illustration of slug size measurement inside microchannel based on slug length, *L*, diameter, *D*, and distance, *d*.

For the total surface area, the individual surface area from a single slug is multiplied with the total number of slugs. Since the channel length is constant, the number of slugs inside the entire microchannel can be estimated by dividing the total microchannel length of 1 m with the domain length, L_d. The calculation method of surface area of a single droplet is based on the slug length, L, and the channel diameter, w, which is equivalent to the channel internal diameter. If $L \leq w$, the surface area is calculated according to Eq. 2 based on Knud Thomsen's approximation of ellipsoidal-like shape.

$$Surface\ area\ (ellipsoidal) \approx\ 4\pi\left(\frac{2\left[\left(\frac{L}{2}\right)\left(\frac{D}{2}\right)\right]^{P}+\left(\frac{D}{2}\right)^{2P}}{3}\right)^{1/P} \tag{2}$$

where $p \approx 1.6075$, L is the slug length, and D is the slug diameter.

If $L > w$, the surface area is calculated according to Eq. 3 based on the approximation of a capsule-like shape.

$$Surface\ area\ (capsule) =\ \mu D^2 + \pi D(L - D) \tag{3}$$

2.5 CFD Simulation and Boundary Conditions

The computational fluid dynamics (CFD) simulation was performed in Ansys Fluent (version 18.2) using the multiphase model of Volume of Fluid (VOF) for tracking the liquid-liquid interface. The solver used was a pressure-based type with a transient time-step. Geometry used was a 3-dimensional domain with the same geometry as the experimental section, and the details are shown in Fig. 3.

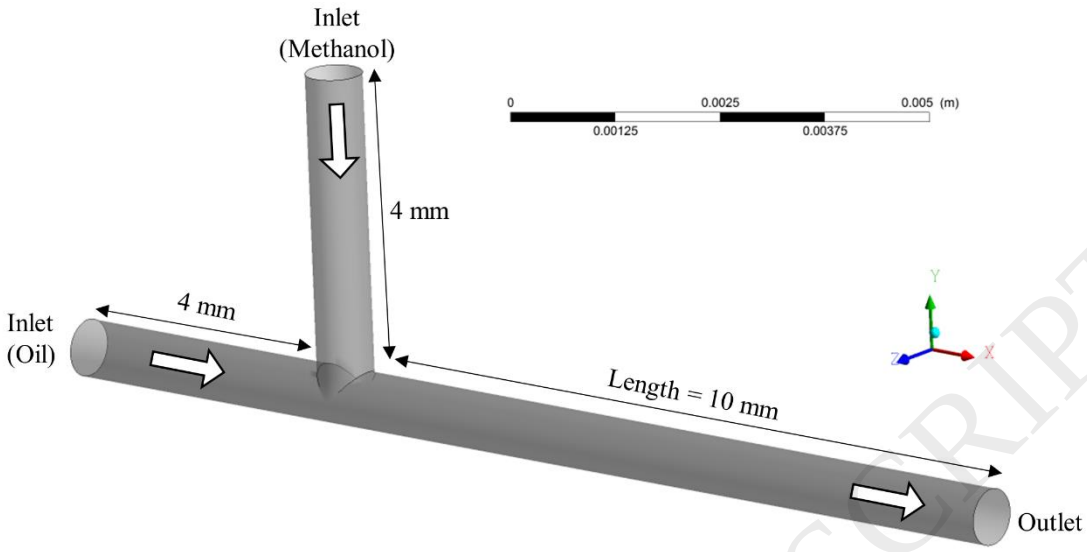

Fig. 3. Geometry description of the microchannel as the 3D simulation domain.

The domain meshing has around 120,000 polyhedral cells and 5-layers of inflation at the wall boudary to improve the result which has been suggested in our previous work (Mohd Laziz and Ku Shaari, 2017). All wall boundaries were applied with a no-slip condition. The time marching of the momentum-continuity equations and the pressure gradient calculations used second-order upwind and least squares cell based gradient calculation schemes, respectively. The continuity equation was solved to separate the phases by tracking the interface between them for volume fraction of one of the phases (ANSYS Inc., 2011). For the q^{th} phase, the continuity equation is shown in Eq. 4; where, $\dot{m}_{qp}$ is the mass transfer from phase q to phase p and $\dot{m}_{pq}$ is the mass transfer from phase p to phase q.

$$\frac{1}{\rho_q}\left[\frac{\partial}{\partial t}\left(\alpha_q \rho_q\right) + \nabla \cdot \left(\alpha_q \rho_q \bar{V}_q\right) = \sum_{p=1}^{n}\left(\dot{m}_{pq} - \dot{m}_{qp}\right)\right] \tag{4}$$

Eq.5 shows the single momentum equation which was solved throughout the domain and the resulting field shared among the phases. The equation is dependent on the volume fractions of all phases through the properties of ρ and μ. The source term $\bar{F}$ in Eq.5 is for the surface tension that uses the continuum surface force (CSF) model. This model was implemented such that surface tension was added to the VOF calculation resulting in a source term in the momentum equation (Brackbill et al., 1992).

$$\frac{\partial}{\partial t}(\rho\bar{v}) + \Delta \cdot (\rho\bar{v}\bar{v}) = -\nabla p + \nabla \cdot [\mu(\nabla\bar{v} + \nabla\bar{v}^T)] + \rho\bar{g} + \bar{F} \quad (5)$$

The pressure drop across the surface depends upon the surface tension coefficient, σ, and the surface curvature as measured by two radii in orthogonal direction, R_1 and R_2, and is presented in Eq. 6

$$p_2 - p_1 = \sigma\left(\frac{1}{R_1} - \frac{1}{R_2}\right) \quad (6)$$

where p_1 and p_2 are the pressures in the two fluids on either side of the interface. Courant number was kept below 0.1 to have a conservative and stable convergent value along the simulation, hence giving the time step in the order of 10^{-5} seconds. The convergence criteria for velocities and pressure was set to be 0.01. Only the result from the case of methanol-to-oil molar ratio of 22.9 at a total volumetric flow rate of 100 μL min^{-1} was taken as an example in the simulation. The boundary conditions for the methanol and oil inlets were both set to be 0.223 cm s^{-1}.

3. Results and Discussion

3.1 Flow Regimes

To observe the hydrodynamic effects of multiphase liquid-liquid flow in a circular microchannel, the volumetric flow rate ratio between methanol and oil was varied. For comparison with the transesterification process, the volumetric flow rate ratio can also be translated to the common reaction parameter of molar ratio. By knowing the density of the liquids and the internal diameter of the microchannel, the molar ratio can be converted to a volumetric flow rate ratio as summarized in Table 1. As the methanol and oil are pumped into the microchannel through the T-junction, a clear distinct two-phase flow regime can be observed, forming a slug flow due to high interfacial forces between the two phases. FEP microchannel wall has superior wettability of the oil phase. Therefore, it created a continuous phase of palm oil that wetted the wall and alternating slug of methanol as the dispersed phase. Depending on the volumetric flow rate ratio of methanol and oil, different slug sizes were observed under an inverted microscope with 2X magnification. The micrograph was then captured by the CCD camera and the results are shown in Fig. 4.

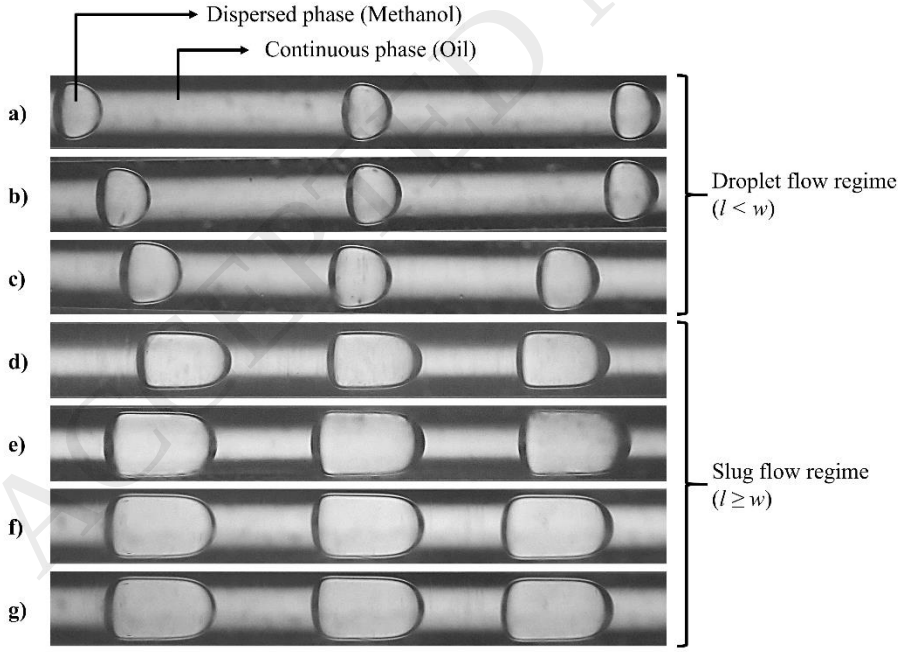

Fig. 4. Micrograph of two-phase flow inside microchannel at methanol-to-oil molar ratio of (a) 3.3, (b) 4.6, (c) 7.6, (d) 10, (e) 15, (f) 20 and (g) 22.9.

From Fig. 4, the flow direction is from left to right in all cases. It is apparent that two different flow regimes prevail at different methanol-to-oil ratios. At this flow rate, the radius of the front slug cap shows higher curvature as compared to the tail slug end that looks flatter than the front droplet cap. This is probably due to the relatively high velocity at a certain *Ca* value which has been described extensively by Li *et* al. (Li and Angeli, 2017). As mentioned earlier, when the slug length is smaller than the microchannel diameter ($l \leq w$), it refers to a droplet flow regime. Slug flow regime is used to describe the slug length larger than the microchannel diameter ($l > w$). At a lower methanol-to-oil molar ratio of 3.3 – 7.6, the flow is in the droplet regime. As the ratio increased to 22.9, the droplet length increases and turns to the slug flow regime due to the increase of its length. Since most of the cases are in the slug flow regime, the term slug instead of droplet will be used to describe the methanol dispersed phase. The total flow rate was constant for all the cases, therefore, a single value of average velocity, Reynolds number, *Re*, and capillary number, *Ca*, can be calculated that are 0.0045 $m.s^{-1}$, 0.04, and 0.09, respectively. The Reynolds number indicates that the flow in the microchannel was in the laminar flow because its value is lower than 2100, which is a common value for all microfluidics cases. According to Xu *e*t al. (Xu et al., 2008), when $0.01 < Ca < 0.3$, the two-phase flow is in the drops flow regime, where the length of dispersed droplet is lower than the width of the channel. In this regime, the cross-flow shear force plays an important role in the process of break-up and its dynamics is dominated by the forces balance between shear force and interfacial force, also known as the dripping regime.

3.2 Droplet Characteristics

To perform a quantitative analysis of the slug characteristics, the inverted microscope equipped with a CCD camera was calibrated to achieve a precise and correct measurement of the

captured micrograph. The slugs were characterized based on the slug length, diameter, and the distance between consecutive slugs. Fig. 5 shows the change in slug length and diameter at different molar flow rate ratios.

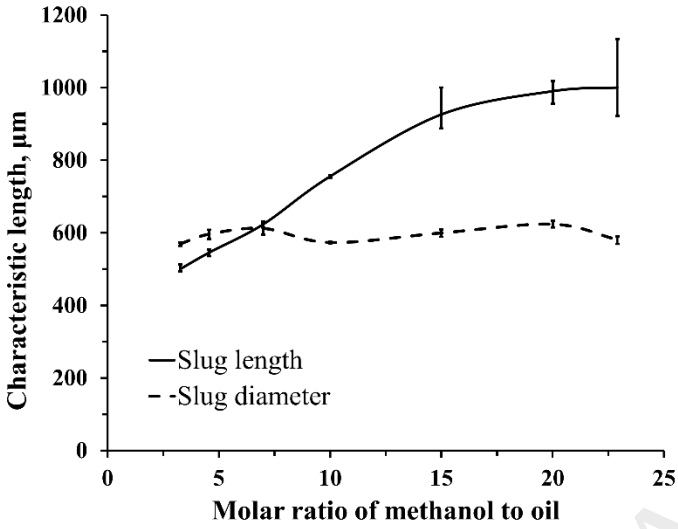

Fig. 5. The characteristic length of slugs at different methanol-to-oil molar ratios

In Fig. 5, most of the error bars show exceptionally small variance with regards to the mean of slug sizes, showing that the slugs remained extremely steady and consistent along the microchannel. Quasi-homogeneous phase was not observed during the transesterification reaction in the microchannel. The formation of steady and consistent slugs was probably due to the accurate flow controller and flow sensors. In addition, the quasi-homogeneous phase or fine droplets, as reported by Guan *et* al. and Rashid *et* al. (Guan et al., 2009; Rashid et al., 2013), were not detected in the current study because the experiment was performed at room temperature. This observation is important to make a correct conclusion based on the hydrodynamic effect on the reaction.

The slug diameter can undergo a maximum increase only up to the size of the microchannel diameter. From this value, the continuous phase film thickness at the wall can be calculated by

deducting the value of microchannel wall internal diameter from the slug diameter. Since the change in slug diameter was very small, therefore the change in diameter is considered insignificant in this study. The slug length, however, clearly shows a linear increase with an increase in the molar ratio and reaches plateau after molar ratio of 20. The typical process of slug formation normally starts with the dispersed phase (methanol) penetrating into the continuous phase (oil) at the junction of the inlet and main channel (Garstecki et al., 2006). Due to the increased pressure in the oil continuous phase, the methanol phase starts to 'squeeze' the neck until it breaks at the rate approximately equal to the mean speed of the oil phase. Before the methanol phase breaks and forms a slug, the slug elongates downstream at the rate of the methanol mean speed. From the Table 1, it can be noticed that the mean speed of methanol was the highest at the higher molar ratio. This suggests that the increase of the slug length is apparently due to the higher flow rate of methanol that elongates during the slug formation at the junction. In addition, the measured slug length from the experiment can be corroborated by the correlation proposed by Xu *et* al. as evident in the Fig. 6 (Xu et al., 2008). The proposed correlation is presented in Eq. 4.

$$\frac{l}{w} = \varepsilon + \omega \cdot \frac{Q_d}{Q_c} \tag{4}$$

where, *l/w* is the dimensionless value of slug length over channel width, ε and ω are the fitting parameters, Q_d and Q_c are the dispersed (methanol) and continuous (oil) volumetric flow rates, respectively. The values of ε and ω are mainly affected by the geometry which give the value of 0.76 and 1.28, respectively.

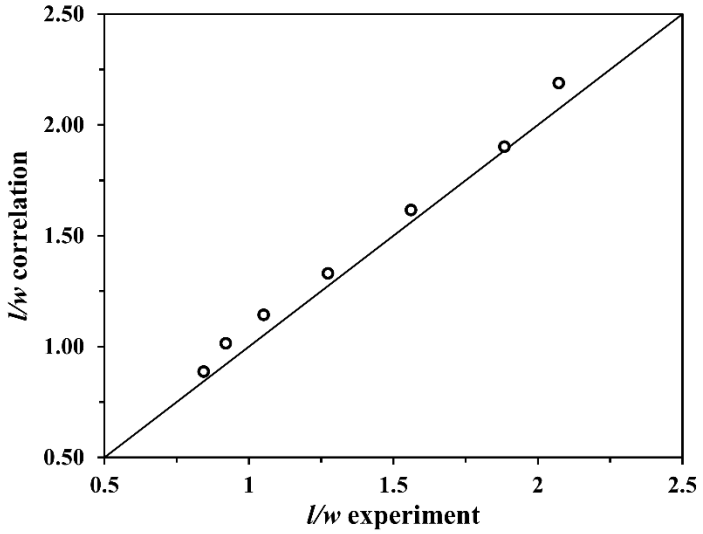

Fig. 6. Comparison of slug length between fitting results from Xu *et* al. correlation and the experimental data.

Another important parameter to study the effect of hydrodynamics on the reaction performance is the number of slugs formed in the microchannel. The number of slugs can be calculated based on the distance from consecutive slugs as described in section 2.4. Fig. 7 shows the distance and the number of slugs at different molar ratios in a 1 m long microchannel.

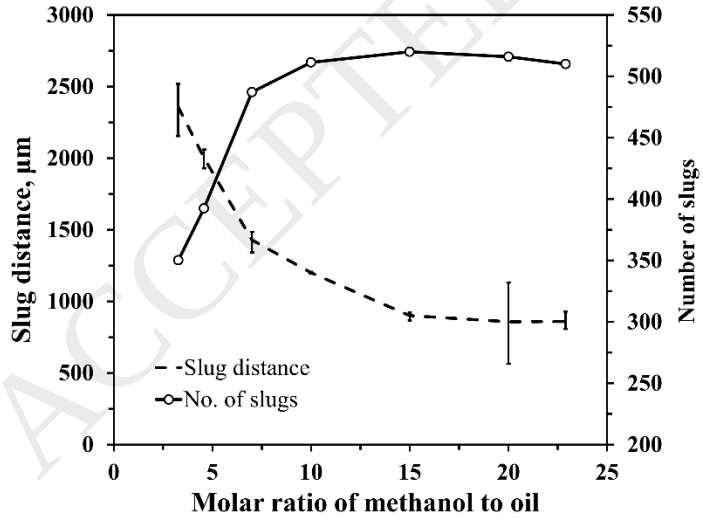

Fig. 7. The slug distance and the calculated number of slugs at different methanol-to-oil molar ratios.

As the molar ratio increases, the slug distance decreases and the number of slugs increases. The number of slugs is hence inversely proportional to the distance between slugs. The reduction in the distance between slugs enable more slugs along the microchannel. The rate of slug formation is related to the mean velocity of both methanol and the oil phases. Despite the constant increment rate of methanol slug length at the higher molar ratio (see Fig.5), the decrement of the slug distance is relatively small as compared to the lower molar ratio (in Fig.7). Therefore, the long slug distance (the lowest molar ratio) is mainly contributed by the high quantity of oil continuous phase and the highest oil inlet flow rate as evident from Table. 1. The number of slugs increases linearly from molar ratio 3.3 to 7.6 due to the linear decrease of distance. However, a further increase of molar ratio did not follow a linear increment because the slug distance decreased marginally due to the increase of slug length.

3.3 Hydrodynamic Effect on the Transesterification Reaction

In multiphase reaction, interfacial area is an important parameter as it is the only area that chemical reaction to take place, limited by the mass transfer at the oil-methanol interface. One way to evaluate the interfacial area is to calculate the surface area-to-volume ratio, *S/V*. Having a stable and consistent slug characteristic is advantageous to calculate the *S/V* ratio more accurately. The reaction performance is evaluated based on the oil conversion from the transesterification process between palm oil and methanol with KOH as a catalyst. The oil conversion was calculated using Eq. 1 based on the amount of TG measured from the sample collected after the reaction. The amount of TG in the sample was measured according to the area under the peak from the HPLC

chromatogram and related with the calibrated value acquired beforehand. Example of chromatogram result at methanol-to-oil ratio of 7.6 is depicted in Fig. 8.

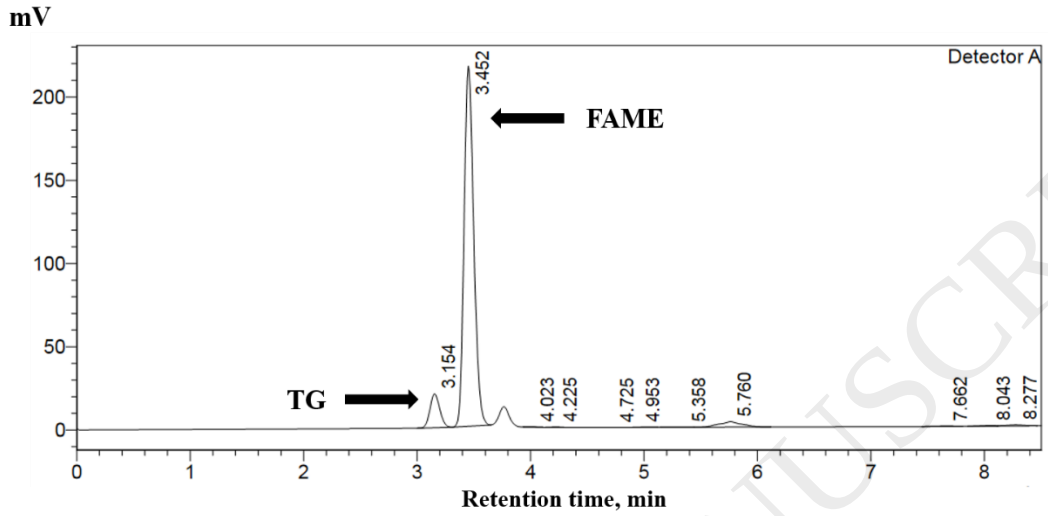

Fig. 8. Chromatogram from HPLC showing the peak of TG and FAME at different retention time for the case of methanol-to-oil ratio 7.6.

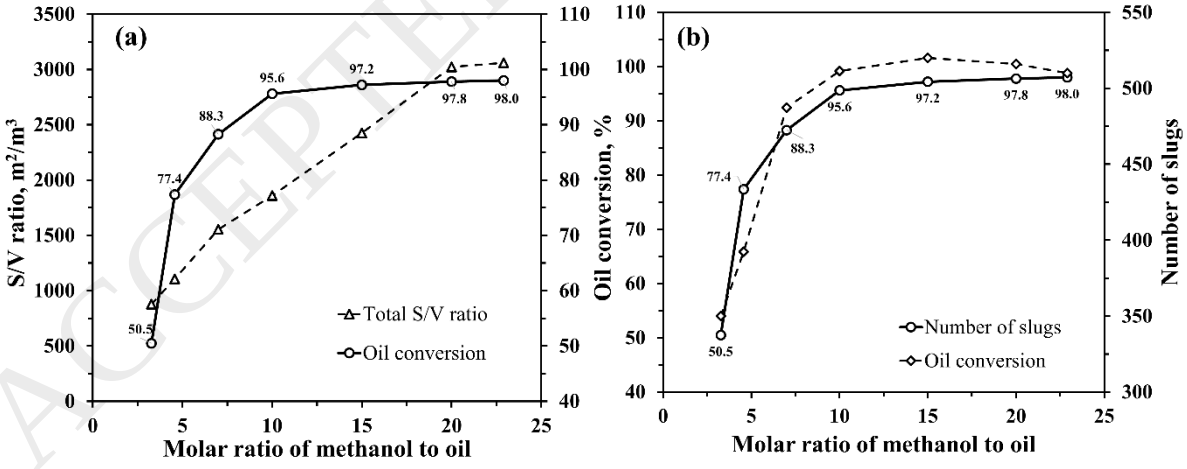

Fig. 9. Comparison between the effect of (a) *S/V* ratio, and (b) number of slugs on the oil conversion. Inset number corresponding to quantitative amount of oil conversion.

Fig. 9 compares the relation of *S/V* ratio and the number of slugs with the oil conversion at different methanol to oil molar ratios. As expected, the oil conversion increases as the molar ratio increases, which has been widely reported in the literature but rarely discussed with the perspective of the hydrodynamic effect. The highest molar ratio of 22.9 results in the maximum oil conversion of 98%, while the lowest molar ratio of 3.3 results in 50% oil conversion. The achievement of 98% oil conversion is remarkably good despite the reaction took place in a mild condition of room temperature and the residence time was as low as 80 seconds only. Therefore, it is evident that this microchannel can produce high quality of biodiesel in an interestingly short amount of time and at the room temperature. In the hydrodynamic perspective, the increase of oil conversion can be linked to the increase of total interfacial area in terms of *S/V* ratio and the number of slugs in the microchannel. The total *S/V* ratio increases linearly as the molar ratio increases suggesting a similar trend with the slug length. The calculated total *S/V* ratio is in the range of 800-3000 m^2/m^3, which is in line with the findings of de Mas *et* al. (de Mas et al., 2005) who used 1 mm polyetheretherketone (PEEK) capillary tubing. Since the volume taken for the calculation of *S/V* ratio was based on the microchannel volume, so the volume was always constant. The only variable that changes the value of *S/V* ratio was the total surface area that was controlled by the slug length. Therefore, it is evident that the trend of *S/V* ratio resembles the trend of slug length. In another perspective of thermodynamics, the increase of methanol-to-oil ratio might influence the solubility of oil into the methanol phase, since the reaction occurs only in the methanol phase. According to the study of Csernica et al., the solubility of TG in the oil increases as the concentration of FAME increases (Csernica and Hsu, 2012). But the FAME exists only when the reaction takes place at the earliest time when both the phases contact each other. Therefore, the FAME is produced in the beginning of reaction at the T-junction where the reaction takes place only at the interface of the

slug. So, the factor that affects the early reaction step is the interfacial area of the slug. The reaction enhances further when FAME is produced and the TG has higher solubility in the methanol, therefore, increases the rate of mass transfer. From this understanding, the different methanol-to-oil ratios have apparently no effect on the solubility of TG in the methanol phase. The result from Fig. 9 shows that, this phenomenon can be achieved through high interfacial area and high oil conversion obtained due to the enhancement of mass transfer and reaction.

However, the number of slugs in Fig.9(b) better matches the oil conversion as compared to the trend of total *S/V* ratio. This hints that the slug number surprisingly shows a closer relation with the oil conversion and it can be an additional factor to the mass transfer and reaction mechanism. To investigate this additional factor, the hydrodynamic inside the slug was further observed at a lower flow rate of 10 μL min^{-1} to easily capture its characteristics. Fig. 10 shows the internal circulation phenomenon inside the methanol slugs at low flow rate condition.

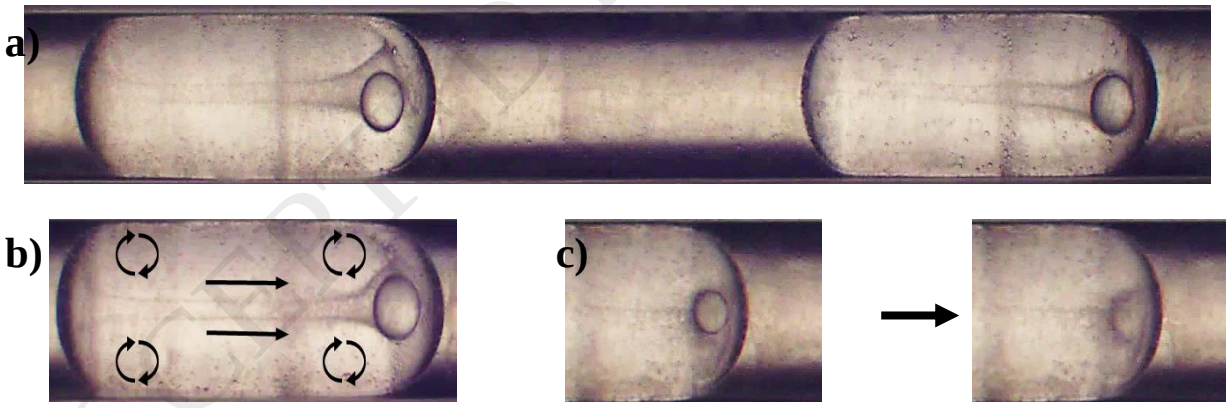

Fig. 10. The micrograph of the methanol slug inside the microchannel at low flow rate; a) original photo; b) with illustration of internal circulation and flow direction; and c) inner FAME droplet burst near to the slug interface.

To observe this phenomenon clearly, a video of the slug flow can be watched in the supplementary data. From Fig. 10(a), a small FAME droplet was observed inside each of the methanol slugs. Due

to the internal circulation, the size of the FAME droplets at the front area of the methanol slug grew with time as illustrated in Fig. 10(b). When the FAME droplet pushed to the interface, it coalesces with the continuous oil phase as shown in Fig. 10(c). This observation can be explained by understanding the phase equilibria between the product FAME and byproduct glycerol with the methanol from the transesterification reaction. Glycerol is a polar compound; therefore, it is fully miscible in methanol (Zhou and Boocock, 2006). Although FAME is non-polar, it is fully miscible in methanol at a very low concentration (Andreatta et al., 2008). However, the mixture will change from single phase to two-phase state after a slightly higher concentration of FAME in methanol. Therefore, the darker contours inside the methanol slug indicate the transformation of one-phase to two-phase FAME-methanol mixture and appear as many tiny droplets (Fig. 10). Since FAME is fully miscible in the oil phase, it dissolves into the oil continuous phase instantaneously once the accumulated FAME droplet at the front methanol region pushes near to the interface as shown in Fig. 10(c).

Interestingly, the internal circulation from the experiment and the accumulation of FAME droplet inside methanol slug were not observed at high flow rate condition of 100 μL min^{-1} as shown in Fig.4. It is more likely due to the mass transfer effect of the FAME component from methanol to oil phase at different flow rates. For the same slug flow regime, high flow rate has better mass transfer as compared to the low flow rate (Biswas et al., 2015; Sattari-Najafabadi et al., 2017). Therefore, at the flow rate of 100 μL min^{-1}, the FAME transfer from the methanol to the oil phase was fast enough, making its concentration in methanol too low to observe the phase change phenomenon that was observed at low flow rate in Fig. 10. Since there was no phase change of FAME in methanol, there was no FAME droplet observed inside the methanol phase. To investigate if the same mixing phenomenon occurred at higher flow rate of 100 μL min^{-1}, a

computational fluid dynamics (CFD) simulation was used. With the help of CFD analysis, the location of the recirculation zones, its velocity, and concentration contour can be observed.

3.4 CFD Simulation

Exact geometry, and flow conditions were implemented in the simulation and validation of the model was performed in previous work that shows good agreement with experimental results (Mohd Laziz and Ku Shaari, 2017). Fig. 11 below illustrates the velocity vector and contour plot of a single slug in the microchannel. The relative velocity was calculated by subtracting the laminar flow profile from the absolute velocity. For circular channel, the laminar flow velocity profile, U_{Lam}, follows Eq. 5, where r is the distance from channel center, and R is channel's radius.

$$U_{Lam} = u(r) = 2V_{Average}\left(1 - \frac{r^2}{R^2}\right) \tag{5}$$

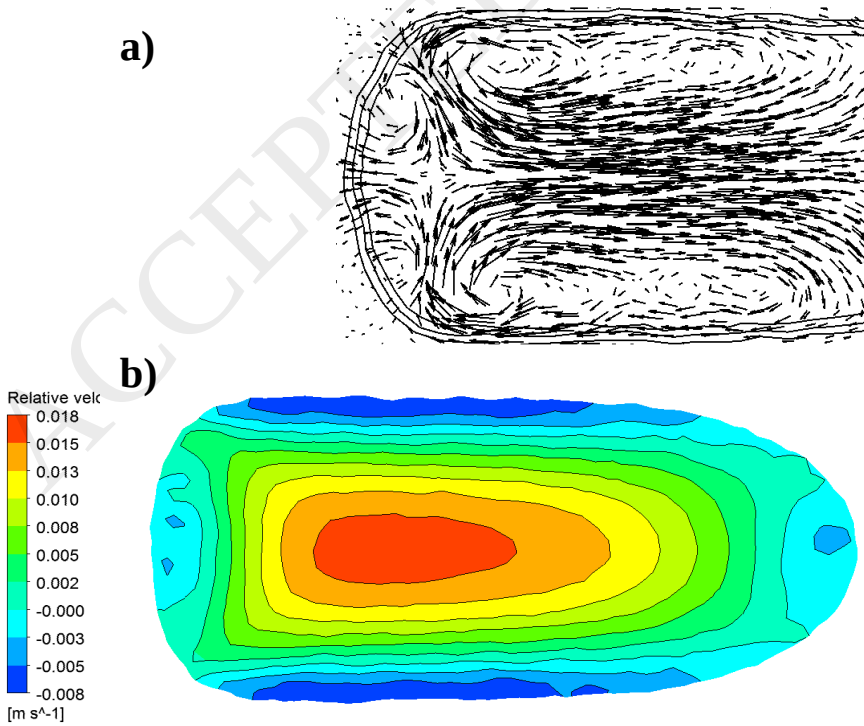

Fig. 11. The simulation results of the flow characteristics inside the slug at the highest molar ratio of 22.9, showing (a) velocity vector, and (b) relative velocity contour plot

From the velocity vector in Fig. 11(a), strong recirculation zones are observed in the slug near the interface that is likely due to the shear forces between the two liquid phases. Compared with the slug at low flow rate, the slug shape at high flow rate becomes flatter at rear and pointier at the front end, which is very similar with the observation from the experimental result from Fig.4(d) discussed earlier. The flow from the recirculation zones pushes everything from the interface area to the inner slug zone. This creates noticeably high velocity flow at the inner zone that moves from the rear to the front zone that can be examined in the velocity contour of Fig. 11(b). The velocity contour plotted here is the relative velocity. Due to the backward flow from the recirculation movement near to the interface, the contour shows negative velocity magnitude which represents the respective velocity magnitude, but only on the opposite flow direction. Most reported recirculation zones in the literature focused on the continuous phase, but in the current study, the focus is on the dispersed phase as an area of interest since the reaction occurs inside the dispersed methanol slug phase. Nevertheless, the recirculation zones presented here are consistent with the results reported in the literature (Li and Angeli, 2017).

The intense mixing inside the slug due to recirculation makes the mass transfer at the interface faster and improves the distribution of oil components throughout the methanol slug. The distribution of partially miscible oil can be observed from CFD analysis as shown in Fig. 12.

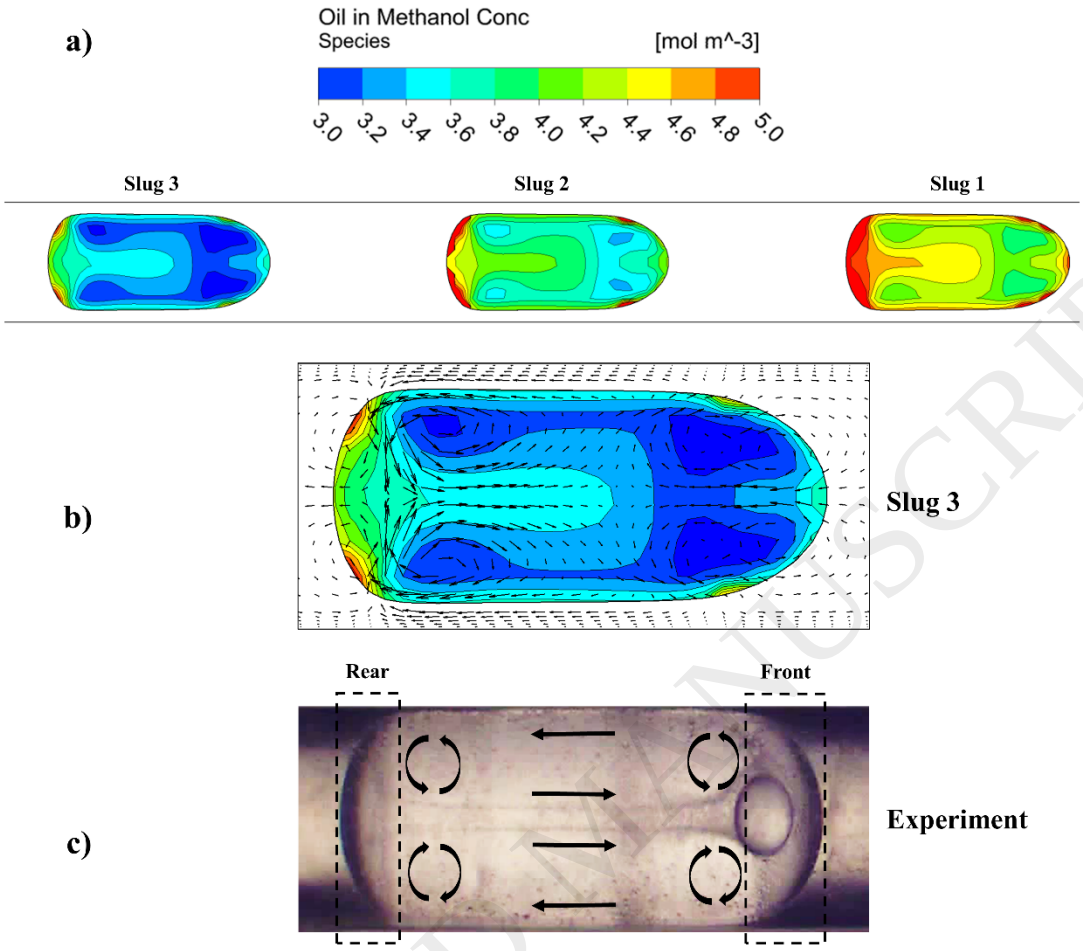

Fig. 12. The contour plot of oil concentration in methanol slug at Q_T=100 μL min^{-1} where (a) three slugs at different position in microchannel, (b) with vector lines, and (c) experimental result with illustration of the hydrodynamics inside the slug.

Fig. 12(a) shows the contour plot of the oil concentration in methanol slugs due to the mass transfer. Three different slugs were captured to observe the development of concentration profile at different residence times. The slug 1 in Fig. 12(a) has the highest oil concentration because it has the longest residence time as compared to the other two slugs. Fig. 12(b) shows the magnified slug 3 with a vector describing the vortices inside the slug. A clear pattern of oil concentration can be observed due to the vortices that are generated by the shearing motion of oil continuous phase. The oil component is transferred into the methanol slug uniformly through the interface boundary.

It is distributed throughout the methanol phase by the mixing effect of the recirculation zones. However, accumulation of oil component in certain region inside the slug can be observed. The highest concentration of the oil is observed at the rear and front end of the slug and moving towards the center. This same phenomenon is observed in the experimental result shown in Fig. 12(c), where the higher concentration regions show darker contours of immiscible FAME formed after the reaction. In addition, the high velocity contour in the middle of the methanol slug shown in Fig. 11(b) explains the high concentration region in Fig. 12(b) where the oil component is distributed from the rear to the center of the slug. The lowest concentration regions are observed inside the vortices as shown in the vector plot Fig. 12(b).

The phenomenon of intense mixing in a single slug can be similarly compared to a batch reactor with impeller where recirculation occurred and help in the mixing process inside the tank as illustrated in Fig.13(a). So, having many slugs inside the microchannel can be visualized as many batch reactors with impellers in series inside the microchannel as illustrated in Fig.13(b). This type of mixing in microchannel is commonly referred as passive mixing (Lee et al., 2011).

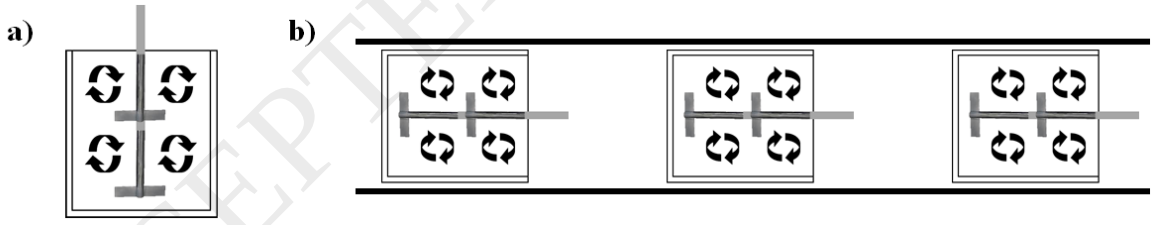

Fig. 13. The illustration of (a) a single tank with impeller, and (b) tilted multiple tanks in series with impeller inside a microchannel.

The increase of methanol-to-oil ratio does not only increase the interfacial area, it also increases the number of slugs created in the microchannel. Due to the existence of internal recirculation zones inside the slug, increase in the number of slugs further enhances the reaction by the effect of passive mixing. Hence, creating more slugs has the advantage in reaction performance for

multiphase flow inside a microchannel. For future study, a more systematic investigation on the mass transfer will be performed that will include mathematical modeling for the relation between mass transfer rate and reaction conversion of the transesterification process.

4. Conclusion

In conclusion, the change of molar ratio changes the hydrodynamic flow characteristics in terms of interfacial area (*S/V*) and the number of slugs. Oil conversion is highest at the highest molar ratio and decreases as the molar ratio decreases. This is due to the increase in the interfacial area and the number of slugs. Most importantly, it has shown that by using a simple 'plug & play' microchannel reactor at room temperature, high conversion of 98% can be achieved. It should be possible, therefore, to produce biodiesel safely and economically at a bigger scale to support the demand of current world energy source.

Acknowledgement

The authors would like to express their appreciation to the Yayasan Universiti Teknologi PETRONAS (YUTP), Chemical Engineering Department, and UTP for the financial and research support, and to Zeus® Germany for providing the ePTFE membrane.

References

Aghel, B., Rahimi, M., Sepahvand, A., Alitabar, M., Ghasempour, H.R., 2014. Using a wire coil insert for biodiesel production enhancement in a microreactor. Energy Convers. Manag. 84, 541–549. https://doi.org/10.1016/j.enconman.2014.05.009

Andreatta, A.E., Casás, L.M., Hegel, P., Bottini, S.B., Brignole, E.A., 2008. Phase equilibria in ternary mixtures of methyl oleate, glycerol, and methanol. Ind. Eng. Chem. Res. 47, 5157–5164. https://doi.org/10.1021/ie0712885

ANSYS Inc., 2011. Fluent 15.0 Theory Guide. Canonsburg, PA.

Billo, R.E., Oliver, C.R., Charoenwat, R., Dennis, B.H., Wilson, P.A., Priest, J.W., Beardsley, H., 2015. A cellular manufacturing process for a full-scale biodiesel microreactor. J. Manuf. Syst. 37, 409–416. https://doi.org/10.1016/j.jmsy.2014.07.004

Biswas, K.G., Das, G., Ray, S., Basu, J.K., 2015. Mass transfer characteristics of liquid–liquid flow in small diameter conduits. Chem. Eng. Sci. 122, 652–661. https://doi.org/10.1016/j.ces.2014.07.029

Brackbill, J.U., Kothe, D.B., Zemach, C., 1992. A continuum method for modeling surface tension. J. Comput. Phys. 100, 335–354. https://doi.org/10.1016/0021-9991(92)90240-Y

Csernica, S.N., Hsu, J.T., 2012. The Phase Behavior Effect on the Kinetics of Transesterification Reactions for Biodiesel Production. Ind. Eng. Chem. Res. 51, 6340–6349. https://doi.org/10.1021/ie300116p

de Mas, N., Günther, A., Kraus, T., Schmidt, M.A., Jensen, K.F., 2005. Scaled-Out Multilayer Gas−Liquid Microreactor with Integrated Velocimetry Sensors. Ind. Eng. Chem. Res. 44, 8997–9013. https://doi.org/10.1021/ie050472s

Elsholkami, M., Cumberland, T., Molyneaux, N., Wei, S., Zambito, N., Elkamel, A., Madhuranthakam, C.M., 2016. Design optimization of a microreactor for the production of biodiesel. Proc. 2016 Int. Conf. Ind. Eng. Oper. Manag. 23–25.

Garstecki, P., Fuerstman, M.J., Stone, H.A., Whitesides, G.M., 2006. Formation of droplets and bubbles in a microfluidic T-junction-scaling and mechanism of break-up. Lab Chip 6, 437–446. https://doi.org/10.1039/b510841a

Guan, G., Kusakabe, K., Moriyama, K., Sakurai, N., 2009. Transesterification of Sunflower Oil with Methanol in a Microtube Reactor. Ind. Eng. Chem. Res. 48, 1357–1363. https://doi.org/10.1021/ie800852x

Jamil, M.F., Uemura, Y., Kusakabe, K., Ayodele, O.B., Osman, N., Majid, N.M.N.A., Yusup, S., 2016. Transesterification of Mixture of Castor Oil and Sunflower Oil in Millichannel Reactor: FAME Yield and Flow Behaviour. Procedia Eng. 148, 378–384. https://doi.org/10.1016/j.proeng.2016.06.487

Lee, C.-Y., Chang, C.-L., Wang, Y.-N., Fu, L.-M., 2011. Microfluidic Mixing: A Review. Int. J. Mol. Sci. 12, 3263–3287. https://doi.org/10.3390/ijms12053263

Li, Q., Angeli, P., 2017. Experimental and numerical hydrodynamic studies of ionic liquid-aqueous plug flow in small channels. Chem. Eng. J. 328, 717–736. https://doi.org/10.1016/j.cej.2017.07.037

Mohd Laziz, A., Ku Shaari, K.Z., 2017. CFD simulation of two phase segmented flow in microchannel reactor using volume of fluid model for biodiesel production, Communications in Computer and Information Science. https://doi.org/10.1007/978-981-10-6463-0_29

Mohd Tamid, A., Ku Shaari, K.Z., Yusup, S., Keong, L.K., 2011. Model Development for Hydrodynamic Study of Fluidized Bed Gasifier for Biomass Gasification. J. Appl. Sci. 11, 2334–2339. https://doi.org/10.3923/jas.2011.2334.2339

Nguyen, T.T., Yee, H.F., Uemura, Y., Mansor, N., 2016. Intrinsic transesterification rate of coconut, palm and sunflower oils with methanol. Sindh Univ. Res. J. 48, 51–56.

Noriega, M.A., Narváez, P.C., Cadavid, J.G., Habert, A.C., 2017. Modeling of biodiesel production in Liquid-Liquid Film Reactors including mass transfer effects. Fuel Process. Technol. 167, 524–534. https://doi.org/10.1016/j.fuproc.2017.08.008

Pontes, P.C., Chen, K., Naveira-Cotta, C.P., Costa Junior, J.M., Tostado, C.P., Quaresma, J.N.N., 2016. Mass transfer simulation of biodiesel synthesis in microreactors. Comput. Chem. Eng. 93, 36–51. https://doi.org/10.1016/j.compchemeng.2016.05.010

Rahimi, M., Aghel, B., Alitabar, M., Sepahvand, A., Ghasempour, H.R., 2014. Optimization of biodiesel production from soybean oil in a microreactor. Energy Convers. Manag. 79, 599–605. https://doi.org/10.1016/j.enconman.2013.12.065

Rashid, W.N.W.A., Uemura, Y., Kusakabe, K., Osman, N.B., Abdullah, B., 2014. Synthesis of Biodiesel from Palm Oil in Capillary Millichannel Reactor: Effect of Temperature, Methanol to Oil Molar Ratio, and KOH Concentration on FAME Yield. Procedia Chem. 9, 165–171. https://doi.org/10.1016/j.proche.2014.05.020

Rashid, W.N.W.A., Uemura, Y., Kusakabe, K., Osman, N.B., Abdullah, B., 2013. Transesterification of Palm Oil in a Millichannel Reactor. J. Japan Inst. Energy 92, 905–908. https://doi.org/10.3775/jie.92.905

Santana, H.S., Silva, J.L., Taranto, O.P., 2019a. Development of microreactors applied on biodiesel synthesis: From experimental investigation to numerical approaches. J. Ind. Eng. Chem. 69, 1–12. https://doi.org/10.1016/j.jiec.2018.09.021

Santana, H.S., Silva, J.L., Taranto, O.P., 2019b. Optimization of micromixer with triangular baffles for chemical process in millidevices. Sensors Actuators B Chem. 281, 191–203. https://doi.org/10.1016/j.snb.2018.10.089

Santana, H.S., Silva, J.L., Tortola, D.S., Taranto, O.P., 2018. Transesterification of sunflower oil in microchannels with circular obstructions. Chinese J. Chem. Eng. 26, 852–863. https://doi.org/10.1016/j.cjche.2017.08.018

Santana, H.S., Tortola, D.S., Reis, É.M., Silva, J.L., Taranto, O.P., 2016. Transesterification reaction of sunflower oil and ethanol for biodiesel synthesis in microchannel reactor: Experimental and simulation studies. Chem. Eng. J. 302, 752–762. https://doi.org/10.1016/j.cej.2016.05.122

Santana, H.S., Tortola, D.S., Silva, J.L., Taranto, O.P., 2017. Biodiesel synthesis in micromixer with static elements. Energy Convers. Manag. 141, 28–39. https://doi.org/10.1016/j.enconman.2016.03.089

Sattari-Najafabadi, M., Nasr Esfahany, M., Wu, Z., Sundén, B., 2017. Hydrodynamics and mass transfer in liquid-liquid non-circular microchannels: Comparison of two aspect ratios and three junction structures. Chem. Eng. J. 322, 328–338. https://doi.org/10.1016/j.cej.2017.04.028

Stankiewicz, A.I., Moulijn, J.A., 2000. Process Intensification : Transfroming Chemcial Engineering. Chem. Eng. Prog. 22–34.

Tanawannapong, Y., Kaewchada, A., Jaree, A., 2013. Biodiesel production from waste cooking oil in a microtube reactor. J. Ind. Eng. Chem. 19, 37–41. https://doi.org/10.1016/j.jiec.2012.07.007

Tiwari, A., Rajesh, V.M., Yadav, S., 2018. Biodiesel production in micro-reactors: A review. Energy Sustain. Dev. 43, 143–161. https://doi.org/10.1016/j.esd.2018.01.002

Wen, Z., Yu, X., Tu, S.-T., Yan, J., Dahlquist, E., 2009. Intensification of biodiesel synthesis using zigzag micro-channel reactors. Bioresour. Technol. 100, 3054–3060. https://doi.org/10.1016/j.biortech.2009.01.022

Xu, J.H., Li, S.W., Tan, J., Luo, G.S., 2008. Correlations of droplet formation in T-junction microfluidic devices: from squeezing to dripping. Microfluid. Nanofluidics 5, 711–717. https://doi.org/10.1007/s10404-008-0306-4

Zhou, W., Boocock, D.G.B., 2006. Phase distributions of alcohol, glycerol, and catalyst in the transesterification of soybean oil. JAOCS, J. Am. Oil Chem. Soc. 83, 1047–1052. https://doi.org/10.1007/s11746-006-5161-4